

Sawdust recycling in the production of lightweight bricks: How the amount of additive and the firing temperature influence the physical properties of the bricks

Giuseppe Cultrone^{*}, Itziar Aurrekoetxea, Carmen Casado, Anna Arizzi

Departamento de Mineralogía y Petrología, Facultad de Ciencias, Universidad de Granada, 18002 Granada, Spain

HIGHLIGHTS

- To study the mineralogy of bricks and to check if it is influenced by the addition of sawdust.
- To determine how the pore system, hydric behaviour and compactness of bricks depend by the amount of sawdust.
- To evaluate the thermal insulation of bricks on the basis of the addition of sawdust and the firing temperature.

ARTICLE INFO

Article history:

Received 26 July 2019

Received in revised form 29 October 2019

Accepted 1 November 2019

Keywords:

Solid bricks

Sawdust

Petrophysics

Thermal insulation

ABSTRACT

This paper studies the influence of sawdust on the petrophysical properties of solid bricks. Brick samples without additives were handmade using a clayey earth that is rich in quartz and phyllosilicates and has some carbonate content. Similar bricks were made with added sawdust at 2.5%, 5% and 10% weight. The bricks were fired in an electric kiln at 800 °C, 950 °C and 1100 °C. The addition of sawdust did not change the mineralogy of the fired bricks. As the firing temperature increased, the quartz content fell and carbonates and phyllosilicates disappeared causing new silicates (gehlenite, wollastonite, anorthite and diopside) to develop. There was an increase in the vitrification of bricks, which also became more compact. At high firing temperature, the bricks had a higher water absorption capacity and worse interconnection between the pores. The high level of vitrification reached at 1100 °C enabled greater transmission of heat inside the bricks. The most refractory bricks were those fired at 800 °C with a 10% sawdust content. When subjected to the salt crystallization test, the most resistant bricks were those with the lowest sawdust content and the highest firing temperature.

© 2019 Elsevier Ltd. All rights reserved.

1. Introduction

The amount of waste produced by industry and households is increasing all the time, while the Earth's capacity to decompose these residues is declining. For this reason, policies encouraging the reuse of waste products are becoming increasingly popular so as to avoid the negative impact on the environment and human health.

A wide variety of research studies have been conducted on the use of waste products as additives in brick manufacture, most of which have focussed on waste products of plant origin such as coal [1], olive pomace [2], mushroom compost waste [3], sugar cane husk and rice hulls [4]. There are also numerous review articles (with extensive bibliography) about the use of additives to

improve the technical quality of bricks [5–8]. The addition of organic substances usually increases the porosity and thermal insulation properties of bricks. In most cases, these are one-off studies which despite promising results have not been applied in large-scale brick production.

Sawdust is one of the organic waste products being tested in a bid to produce bricks with enhanced heat insulation properties. If we bear in mind the volume of trees that are felled every year (over 400 million m³ since the year 2000 in the European Union, <https://ec.europa.eu/eurostat/>) in the production of firewood for fuel, sawn wood, veneers, pulp and paper, one can imagine the huge amounts of sawdust generated during sawing. In chemical terms, sawdust is composed approximately of 60% carbon, 34% oxygen, 5% hydrogen and 1% nitrogen [9]. The organic polymers of which it is composed are essentially cellulose and lignin. Wood is often treated with varnishes and resins, both during sawing and storage, so as to guarantee better conservation. Sawdust from wood treated

^{*} Corresponding author.

E-mail address: cultrone@ugr.es (G. Cultrone).

in this way is more difficult to recycle [10]. As well as creating a problem of storage space, sawdust can pollute land and water. It normally retains a high moisture content allowing the development of different species of fungi which later spread to nearby vegetation causing it to rot. This is why the best option is to reuse sawdust to make other materials [11]. Sawdust typically has variable grain sizes, colours and consistencies depending on the type of wood being sawn. Only a small amount of sawdust is recycled in for example the manufacture of chipboard panels, the cleaning of wet floors and most recently in the production of pellets for use as fuel in boilers. As regards the addition of sawdust in brick production, by itself or mixed with other organic additives, research has shown that higher quality bricks are obtained at high firing temperatures because the sintering process increases the resistance of bricks to compression [9,12]. The addition of sawdust to clay mixtures also seems to reduce the interconnection between the pores in fired bricks [13]. When different concentrations of sawdust were tested, the best physical and mechanical results were obtained with low percentages of waste [14]. Arsenović et al. [15,16] found that the organic additives tested in the production of roof tiles, solid bricks and hollow bricks led to a higher water absorption capacity and less mechanical resistance and that the best results with sawdust were obtained when it was used in the production of solid bricks. In research on other waste products that could perform similarly to sawdust when added to bricks, Sena da Fonseca et al. [17] observed that the incorporation of spent coffee grounds obtained from the brewing process increased thermal insulation (the addition of just 5% of this waste product increased the thermal insulation of bricks by 30%). However, the addition of coffee grounds increased the water absorption content and reduced the compressive strength, so making it more difficult to use these bricks for construction purposes [18]. Ozturk et al. [19] observed that the addition of tea waste in quantities of over 10% to bricks fired at 950 °C and 1050 °C reduced their mechanical strength so that they could only be used for thermal insulation purposes. In all these studies, the addition of organic wastes produced more porous bricks, although their durability with a view to possible use in construction was not assessed.

As can be seen from the literature, the research on sawdust and its influence on the physical properties of bricks is quite limited. Therefore, the aim of this research is to evaluate how the addition of this waste product influences the petrophysical properties of handmade solid bricks. The use of sawdust as an additive in brick manufacture could offer an environmentally-friendly alternative for the production of bricks with specific physical properties. Its use can generate some economic benefits due to: a) less extraction, transport and preparation of the required raw material which is partially replaced by waste; b) reduced need for disposal/landfilling of waste; c) additional indirect social, economic and environmental benefits due to the recycling of such waste material and the preservation of non-renewable clay resources. One environmental drawback of using sawdust as an additive in brick production is increased emission of CO₂ into the atmosphere when the sawdust is burnt during firing. This would be in addition to the CO₂ already emitted by brick factories due to natural gas combustion and due to the decomposition of the carbonates and the destruction of the organic matter contained in the clayey materials [20]. It is important to stress however that additional carbon dioxide emissions will be an issue for any alternative for the reuse of sawdust that involves incineration [17]. In this research a series of analytical techniques were performed to assess and compare the technical quality of the bricks made without additives and those made with differing percentages of added sawdust. Possible changes in their mineralogy and texture were evaluated by means of X-ray diffraction and scanning electron microscopy, while their porous system and density were analysed using hydric tests and

mercury intrusion porosimetry. The relative compactness of the different samples was assessed using ultrasounds. The samples were also subjected to the salt crystallization test to study their durability, and their colour and insulating properties were analysed using spectrophotometry and IR thermography, respectively, so as to optimize their performance.

2. Materials and methods

2.1. Preparation of the brick samples

The clayey earth used to make the bricks comes from a quarry in Jun, a village near Granada in southern Spain. In geological terms, this area falls within the intramountain basin of the Betic Cordillera and is covered by Neogene and Quaternary materials from the depression of Granada. It is occupied by sediments composed of lacustrine series of grey clays, micaceous silts and sands from the Messinian Age, occasionally interspersed with bands of gypsums and conglomerates [21]. At present, this clayey earth is quarried by a local brick factory (<https://www.ceramicacastillosiles.es/>) which manufactures and markets tiles and bricks using both industrial (by extrusion) and artisanal production methods.

The waste product used as an additive was beechwood sawdust from the carpentry workshop in the Faculty of Sciences at the University of Granada (Spain). This sawdust is the same as that produced in large quantities by industrial manufacturers of wood products and amassed in factories. The sawdust was sieved to remove the larger grains, leaving those of less than 1.5 mm which were then kneaded in with the clayey earth. The sawdust particles were quite uniform in size and generally oblong in shape. There is no standard figure for the amount of sawdust that should be added to the bricks. For example, Chemany & Chemany [9] tested the sawdust from eucalyptus and pine trees in percentages of between 3% and 9% in weight, while Demir [14] added a mixture of organic residues (sawdust, tobacco and grass) in increasing temperatures up to 10% in weight. In this research the textural and physical changes undergone by bricks as a result of the addition of sawdust in concentrations of 2.5%, 5% and 10% in weight were investigated.

The brick samples used in this research were handmade using an artisanal process. Although the vast majority of the bricks produced today are industrially manufactured by extrusion, handmade bricks are more appropriate in cases in which less standardized products are required. Indeed, there is a clear demand from architects, builders and restorers for bricks of varying sizes, shapes and finishes for use in the construction of new houses in traditional style and in the restoration of historic buildings [22]. Artisanal bricks also have another advantage over extruded ones as they offer greater flexibility in terms of the number of units produced, which produces savings in the use of raw materials [23]. The first stage of this artisanal process was to sieve the clayey earth so as to remove fragments of over 1.5 mm in size, amongst which gypsum crystals could be easily identified. The samples with no additive were prepared by kneading 1.6 kg of clayey earth with 450 ml of water. Once sufficient plasticity had been achieved, the ceramic paste was placed in a moistened wooden mould measuring 15 × 20 × 4 cm³. The mould was filled gradually, starting with the corners, until completely full. The paste was then pressed down by hand. The surface of the paste was smoothed down with a previously moistened plastic ruler. After an hour the still moist brick paste was removed from the mould and cut into 4 cm-edge cubes using cotton thread stretched tight. The same process was followed for the bricks with added sawdust. The only difference being that the amount of clay was reduced and the amount of sawdust increased on the basis of the percentage of sawdust used in each case (Table 1). Three moulded samples were prepared from each kneaded mixture, so that they could be fired at three different firing temperatures (800 °C, 950 °C and 1100 °C). These three temperatures were chosen on the basis that 950 °C is one of the most commonly used temperatures in brick production. The other two firing temperatures were chosen to enable us to study the textural and physical changes that take place in the bricks over a 300 °C temperature range. Table 1 shows the acronym assigned to each brick sample on the basis of the amount of added sawdust and the firing temperature. Before firing, the raw unfired samples were left to dry out for about a week in the laboratory at a temperature of 25 °C and 50% relative humidity.

Samples were fired in a Herotec CR-35 electric kiln. Since there is no specific standard for the firing process, similar heating and cooling times to those cited in previous research were followed [24]. The temperature inside the kiln was kept constant at

Table 1
Acronym assigned to each sample based on the amount of sawdust and the firing temperature.

Sawdust (%)	800 °C	950 °C	1100 °C
0	J800	J950	J1100
2.5	J800-A	J950-A	J1100-A
5	J800-B	J950-B	J1100-B
10	J800-C	J950-C	J1100-C

100 °C for 1 h so as to eliminate any residual moisture that might be left in any of the samples. The samples were then heated up to the pre-set maximum firing temperature (800 °C, 950 °C or 1100 °C) at a heating speed of 2 °C/min. Once this maximum temperature had been reached, it was maintained for 3 h. Finally, the kiln was turned off and the bricks were left to cool until the next day, with the whole firing-cooling process taking about 24 h. This slow cooling process prevented possible cracking of bricks caused by β -quartz to α -quartz transition and it was therefore not necessary to temporarily halt the process at 573 °C. Given that, on the basis of previous geological evidence [21], it was highly likely that the clayey earth raw material contained carbonates, when the bricks were taken out of the kiln, they were submerged in water for one hour to eliminate the grains of CaO. This precaution is essential given that calcite starts to decompose into CaO and CO₂ at around 600 °C [25]. Calcium oxide reacts quickly with moisture and is converted into portlandite (Ca(OH)₂) in an exothermic reaction. The increase in volume brought about by the crystallization of portlandite and its subsequent carbonation into calcite causes the bricks to break ("lime blowing", according to Laird and Worcester [26]). Indeed, after the samples were immersed in water, a white film began to form on the surface of the water due to the carbonation of the grains of CaO in the bricks.

2.2. Analytical techniques

2.2.1. Chemism, mineralogy and texture

The chemical composition of the raw material and the fired samples in terms of major oxides (SiO₂, Al₂O₃, Fe₂O₃, MnO, MgO, CaO, Na₂O, K₂O, TiO₂ and P₂O₅ in wt%) and trace elements (Zr, V, Cr, Ni, Zn, Ba, Pb, Rb, Sr and Y in ppm) was determined by X-ray fluorescence (XRF) using a PANalytical Zetium compact spectrometer with Rh anode and 4 kV X-ray generator. 7 g per sample were milled to powder in an agate mortar and then analysed.

The mineralogy of the raw material and the bricks was determined by X-ray diffraction (XRD) with a PANalytical X'Pert PRO diffractometer using disoriented powder samples. The following working conditions were used: CuK α radiation, 45 kV voltage, 40 mA current, 3 to 60° 2 θ exploration range, 0.1 2 θ s⁻¹ goniometer speed. Mineral phases were identified using the X'Pert software programme [27]. The analysis of mineral phases was performed using the non-linear least square method to fit full-profile diffractograms and the results were compared with standard values in the database. The American Mineralogist Crystal Structure Database (AMCSD) was used to identify the mineral phases. An indicative value of the amorphous versus crystalline phases (a/c) ratio was provided. This ratio is based on the mean value of the intensities, standard deviation and area of the crystal reflection [27].

Small carbon-coated fragments from brick samples were observed under a high-resolution environmental scanning electron microscope (FEG-ESEM) Quanta 650F operating at 5 kV in order to observe changes in the mineralogy and texture of bricks as a consequence of the firing temperature and the addition of sawdust. Energy dispersive X-ray (EDX) analysis was used for elemental analysis of crystals within the fragments.

2.2.2. Study of the porous system

Hydric tests were performed to quantify the absorption and drying capacity of the bricks over time. These tests can provide indirect information about the durability of construction materials in that many decay processes involve the flow of water through pores and fissures [28]. Free (A_b) and forced water absorption (A_r) and drying (Di) tests were carried out according to the UNE-EN 13755 [29] and NORMAL 29/88 [30] standards, respectively. These tests evaluated the degree of pore interconnectivity (A_x, [31]), the saturation coefficient (S), the apparent (p_a) and real densities (p_r) and the open porosity (P_o) according to the RILEM standard [32]. Hydric tests were performed under controlled thermo-hygrometric conditions (18 °C and 35% relative humidity) using deionized water. Three samples per brick group were analysed.

The characterization of the porous system of bricks was completed with mercury intrusion porosimetry (MIP) using a Micromeritics Autopore IV 9500 porosimeter. The pore size distribution was analysed within a range of between 0.002 and 200 μ m. One sample per brick type of about 1 cm³ was oven-dried at 70 \pm 5 °C for 8 h before being analysed. The specific surface area (SSA), open porosity (P_{oMIP}) and apparent and real densities (P_{aMIP} and P_{rMIP}) were also calculated.

2.2.3. Compactness, colour and thermal conductivity

Ultrasound, spectrophotometry and IR thermography are particularly useful techniques as they are non-destructive. Ultrasound offers information about the compactness of materials and analyses their structural anisotropy and provides indirect information about the strength of bricks [33,34]. Measurements were carried out using a Controls 58-E4800 ultrasonic pulse velocity tester with 54 kHz transducers. Three samples per brick type were measured. An eco-gel was used to obtain a good coupling between the transducers and the surface of the bricks. The propagation of P-waves was measured using the transmission method according to the ASTM D2845 standard [35] in dry samples. The structural (Δ M) and relative anisotropies (Δ m) were calculated according to the following equations [36]:

$$\Delta M = \left(1 - \frac{2V_{P1}}{V_{P2} + V_{P3}} \right) \times 100$$

$$\Delta m = \frac{2(V_{P2} - V_{P3})}{V_{P2} + V_{P3}} \times 100$$

where V_{P1}, V_{P2} and V_{P3} are the velocities measured in the three orthogonal directions.

The colour of the brick surfaces was measured by spectrophotometry using a portable Konica Minolta CM-700d apparatus in accordance with the UNE-EN 15886 standard [37]. CIE illuminant D65 (simulating daylight with a colour temperature of 6504 K) was selected to measure the lightness (L*) and chromatic coordinates (a* and b*) in the 400–700 nm wavelength range. The illumination was provided by a pulsed xenon lamp with a UV cut filter and the light was detected and measured using a silicon photodiode array in SCI and SCE modes. An area of 8 mm in diameter (10° vision angle) per sample was analysed. Three measurements were carried out per brick type. The colour difference (ΔE) due to the addition of sawdust was calculated as follows:

$$\Delta E = \sqrt{(L_1^* - L_2^*)^2 + (a_1^* - a_2^*)^2 + (b_1^* - b_2^*)^2}$$

where L₁^{*}, a₁^{*}, b₁^{*} are the lightness and chromaticity values for the bricks made without additives and L₂^{*}, a₂^{*}, b₂^{*} for those made with added sawdust.

A qualitative estimation of the heat propagation inside the bricks was measured by IR thermography. This technique converts thermal radiation into electric signals that produce a visible image. A FLIR T440 thermographic camera was used in the laboratory where thermo-hygrometric conditions were maintained constant (25 °C and 50% relative humidity). Brick cubes were heated on a hot plate at 50 °C for 30 min at a distance of 30 cm from the camera lens. The propagation of heat along the surface of the bricks was recorded every minute on IR thermographic images and the displacement of the 50 °C isotherm was measured.

2.2.4. Durability by salt crystallization

The bricks were subjected to the salt crystallization test according to the UNE-EN 12370 [38] standard. This test provides information on the damage produced by the crystallization in pores and fissures of salts that are usually dissolved in water. 15 cycles were performed on three bricks of each type using a 14% Na₂SO₄ × 10H₂O solution that can exert a crystallization pressure of 14 MPa in confined spaces [39]. The gradual deterioration of the bricks was evaluated by visual inspection and daily weight measurement.

A list of the analytical techniques used in this paper is set out in Table 2.

3. Results

3.1. Chemism, mineralogy and texture

In chemical terms, the clayey earth from Jun is rich in silica and aluminium. It also has significant quantities of calcium, iron and magnesium in that order (Table 3). CaO and MgO content is well above 6%, which means that the clay can be classified as calcareous [40]. As might be expected, the firing does not alter the concentration of major and trace elements. The most abundant trace

Table 2

Summary of the techniques used to carry out this research and the number of analyses performed per brick type. Legend: XRF = X-ray fluorescence; XRD = X-ray diffraction; FEG-ESEM = field emission gun environmental scanning electron microscope; MIP = mercury intrusion porosimetry; IR = infrared.

Technique	Apparatus	Norm	Analyses per brick type
XRF	PANalytical Zetium		1
XRD	Panalytical X'Pert Pro		1
FEG-ESEM	Quanta 650F		1
Hydric tests		UNE-EN 13755 [29] NORMAL 29/88 [30] RILEM [32]	3
MIP	Micromeritics Autopore IV 9500		1
Ultrasounds	Controls 58-E4800	ASTM D2845 [35]	3
Spectrophotometry	Konica Minolta CM-700d	UNE-EN 15886[37]	3
IR thermography	FLIR T440		1
Salt crystallization		UNE-EN 12370[38]	3

Table 3
Chemical analysis of the major oxides (in wt%) in the clayey earth raw material (J) and the fired bricks. LOI stands for loss on ignition. Brick abbreviations are indicated in Table 1.

	SiO ₂	Al ₂ O ₃	Fe ₂ O ₃	MnO	MgO	CaO	Na ₂ O	K ₂ O	TiO ₂	P ₂ O ₅	LOI
J	48.46	16.16	5.81	0.06	3.36	8.96	0.62	2.77	0.77	0.13	13.16
J800	50.05	15.74	5.63	0.08	4.07	11.66	0.81	2.89	0.73	0.14	5.49
J800-A	48.90	15.51	5.57	0.07	4.00	11.47	0.8	2.83	0.72	0.13	7.49
J800-B	48.82	15.15	5.42	0.08	5.07	12.38	0.63	2.88	0.71	0.13	6.99
J800-C	47.39	15.89	5.76	0.09	5.15	13.56	0.59	3.02	0.71	0.14	6.72
J950	50.94	16.17	5.79	0.08	4.25	12.26	0.84	2.99	0.76	0.14	2.35
J950-A	51.71	16.40	5.79	0.08	4.28	12.26	0.82	3.02	0.76	0.14	2.09
J950-B	51.23	15.89	5.63	0.08	5.24	12.97	0.70	3.01	0.74	0.14	1.90
J950-C	51.28	16.10	5.71	0.08	5.33	13.15	0.69	3.04	0.74	0.14	2.21
J1100	52.04	16.50	5.87	0.08	4.22	12.12	0.82	2.99	0.77	0.14	1.22
J1100-A	51.66	16.14	5.71	0.08	5.39	13.12	0.67	3.04	0.76	0.14	0.61
J1100-B	51.63	16.10	5.68	0.08	5.35	13.25	0.67	3.01	0.74	0.14	0.65
J1100-C	52.18	16.39	5.83	0.09	5.44	13.32	0.70	3.01	0.74	0.14	0.89

elements include barium, strontium and zirconium (Table 4), which may indicate the presence of barite, celestine and zircon as accessory minerals. The only significant change is the loss on ignition (LOI, Table 3). LOI is slightly higher in the clay raw material (13%) than in bricks, which together with the organic material contain phyllosilicates, carbonates and sulphates that lose H₂O and CO₂ after calcination. The addition of sawdust in its different amounts did not alter LOI, in that the same evolution was observed in all four groups of bricks. The highest values were measured at 800 °C when there may still be carbonates which lose their CO₂, while at 950 °C and 1100 °C, there was only minimum loss associated with a residual dehydroxylation of the phyllosilicates. On this question, Rodríguez Navarro et al. [41] demonstrated that the dehydroxylation of muscovite remains incomplete at 950 °C. The results of the mineralogy set out below confirm these suppositions.

In mineralogical terms, the clayey earth from Jun is rich in quartz and phyllosilicates (above all illite/muscovite and also paragonite, chlorite and kaolinite), feldspars *s.l.* (microcline and albite), gypsum and carbonates (calcite and dolomite) (Table 5). After firing at 800 °C, quartz is still the most abundant mineral while phyllosilicates disappear, with the sole exception of illite/muscovite, which remains present albeit in lower concentrations (Table 5). Of the carbonates, dolomite is no longer detected and calcite is present but in smaller quantities than in the raw material. Microcline is transformed into orthoclase, the most stable polymorph at this temperature. Gypsum loses its water molecules and is converted into anhydrite (Table 5). At 950 °C calcite and quartz disappear and the concentrations of illite/muscovite are lower. In addition, new mineral phases are formed by the reaction between silicates and carbonates. One example is gehlenite, which is produced by the reaction between calcite and illite/muscovite [24]. Plagioclases turn into anorthite and orthoclase changes into its higher-temperature phase, sanidine (Table 5). At 1100 °C quartz

is no longer the main mineral phase as anorthite is present in larger concentrations. Two other silicates, wollastonite and diopside, appear due to the quartz reacting with calcite and dolomite respectively [42]. The amount of gehlenite falls because it is also involved in the formation of wollastonite [42]. Illite/muscovite is no longer detected (Table 5). The amount of hematite remains approximately the same. In addition, as the firing temperature increases so does the amorphous/crystalline ratio (a/c, Table 5) due to the gradual vitrification of the bricks.

The addition of sawdust does not change the mineralogy compared to the bricks without additives, in that the same phases are identified and the same reactions take place: carbonates decompose, muscovite-type phyllosilicates lose the hydroxyls (OH⁻) and disappear above 950 °C, the concentration of quartz falls forming gehlenite, anorthite, wollastonite and diopside (Table 5). It is interesting to note that the amount of amorphous phase does not increase in the presence of sawdust, nor does the amorphous/crystalline ratio (a/c, Table 5). On this question, Demir [14] noted that the addition of organic matter to the bricks produced extra heat during firing in the kiln and Dondi et al. [43] quantified the calorific value of sawdust at around 17,000 kJ/kg. We should remember however that the sawdust burns at relatively low firing temperatures (between 200 °C and 650 °C according to Guo et al. [44]), which means that its addition to the clayey matrix cannot contribute to vitrification or to the increase in the amorphous phase, which take place at higher firing temperatures.

ESEM observations were only conducted in the bricks without additives and in those with 10% added sawdust fired at 800 °C and 1100 °C for which the textural differences were more evident. In bricks made without additives the level of vitrification of bricks increases in line with increasing firing temperature. At 800 °C the sheet habit of phyllosilicates remains, the bond between the grains seems limited and pores have a clearly angular shape (Fig. 1a).

Table 4
Chemical analysis of the trace elements (in ppm) in the clayey earth raw material (J) and the fired bricks. Brick abbreviations are indicated in Table 1.

	Zr	V	Cr	Ni	Zn	Ba	Pb	Rb	Sr	Y
J	219	70	82	38	78	325	33	126	326	70
J800	203	97	81	37	88	365	190	131	699	97
J800-A	202	76	79	39	89	357	37	129	671	76
J800-B	201	67	78	40	88	367	36	132	394	67
J800-C	176	79	77	43	89	379	32	138	481	35
J950	218	79	146	49	95	376	37	134	769	79
J950-A	212	82	84	40	95	392	36	136	757	82
J950-B	201	71	78	39	90	387	37	135	489	71
J950-C	207	76	81	38	87	389	30	136	482	36
J1100	217	71	84	41	9	392	33	134	727	71
J1100-A	213	82	83	40	91	349	39	135	418	82
J1100-B	206	77	99	44	93	382	33	134	461	77
J1100-C	205	75	89	36	89	406	27	135	465	37

Table 5

Mineralogical composition of raw material (J) and fired bricks. Legend: **** = very abundant; *** = abundant; ** = small quantities; * = scarce; tr = in traces. Qz = quartz; Ms = illite/muscovite; Pg = paragonite; Chl = chlorite; Kao = kaolinite; Cal = calcite; Dol = dolomite; Gyp = gypsum; Anh = anhydrite; Hem = hematite; Mic = microcline; Or = orthoclase; Sa = sanidine; Ab = albite; An = anorthite; Gh = gehlenite; Di = diopside; Wo = wollastonite; a/c = amorphous/crystals relationship. Mineral abbreviations after Whitney and Evans [45]). Brick abbreviations are indicated in Table 1.

	J	J800	J800-A	J800-B	J800-C	J950	J950-A	J950-B	J950-C	J1100	J1100-A	J1100-B	J1100-C
Qtz	****	****	****	****	****	****	****	****	****	***	***	***	***
Ms	***	**	*	*	**	*	tr	tr	*				
Pg	**												
Chl	*												
Kao	*												
Cal	*	*	*	*	*								
Dol	*												
Gyp	*												
Ahn		*	*	*	*	*	**	*	tr	*	*	tr	*
Hem		tr	tr	tr	tr	tr	tr	tr	tr	tr	tr	tr	tr
Mic	**												
Or		**	**	**	***								
Sa						**	**	**	**	*	*	*	tr
Ab	*	**	**	**	**								
An						***	***	***	***	****	****	****	****
Geh						**	**	**	*	*	*	*	*
Di										**	**	**	**
Wo										**	**	**	**
a/c	0.089	0.059	0.061	0.068	0.084	0.066	0.090	0.090	0.072	0.108	0.143	0.093	0.112

At 1100 °C the texture was quite different, vitrification was much more widely extended and the pores coalesced becoming spherical or oval-shaped (a “cellular structure” according to Tite and Maniatis [46]) (Fig. 1b). This was due to the melting of clay particles and the release of gases [47]. These observations confirm that the increase in the amount of amorphous phase deduced by XRD (a/c, Table 5) in line with increasing firing temperature is due to the vitrification of the bricks. On occasions it is possible to observe the remains of former carbonates which have decomposed into oxides and have not carbonated after the immersion of the brick samples in water. Indeed, the detail image in Fig. 1c shows a grain composed of equidimensional nanometric Mg oxides (see the EDX

spectrum) with rounded edges, probably after undergoing sintering, which makes their reaction to form new silicates more difficult [25,48]. Anhydrite grains with pronounced exfoliation due to the loss of H₂O during the transformation of the gypsum into anhydrite were also identified (Fig. 1d).

The addition of sawdust gives rise to new elongated pores, which are larger than those observed earlier and were formed after combustion of the organic matter leaving the imprint of the original shape (Fig. 1e). At this temperature there are no signs of vitrification of the matrix. At 1100 °C the same pores are visible although the edges are smoother, the smallest pores are rounder and, in general, the structure seems to be more compact (Fig. 1f).

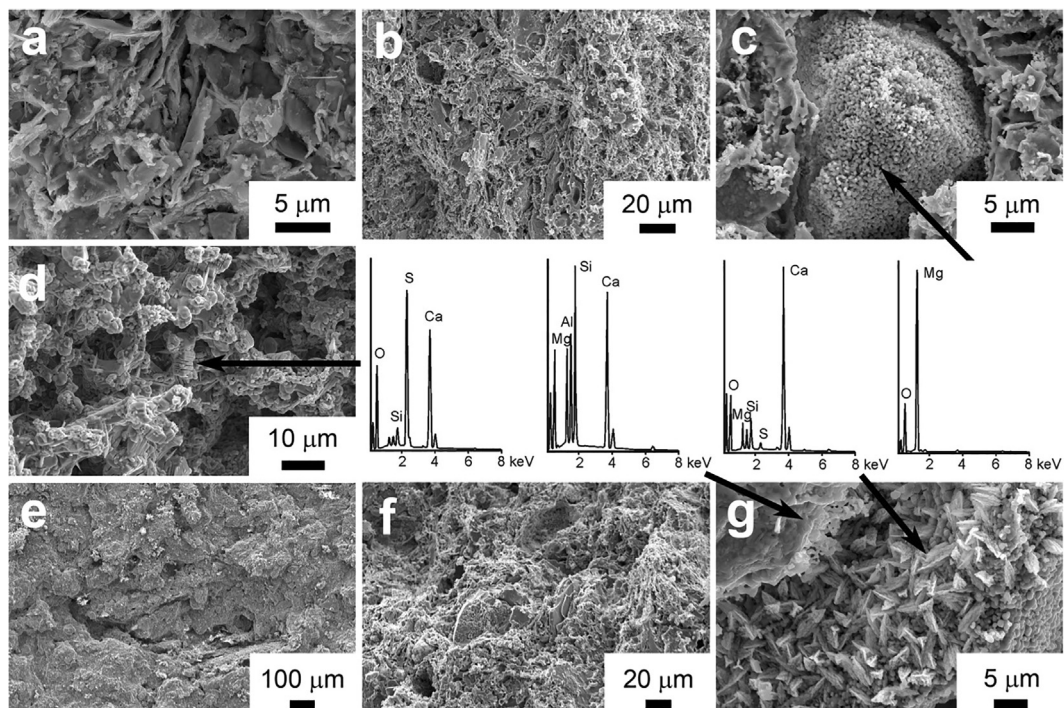


Fig. 1. ESEM secondary electron images and EDX microanalysis of bricks without additives (images a, b, c and d) and with the addition of 10 wt% sawdust (images e, f and g), fired at 800 °C (images a and e) and at 1100 °C (images b, c, d, f and g).

The crystals with a trigonal habit and rough surfaces on the pore in Fig. 1g were identified as calcite (see the EDX spectrum). This mineral phase is incompatible with firing temperatures of 1100 °C and is a secondary calcite. This calcite was formed after firing when the samples were submerged in water so as to prevent lime-blowing (see above - Preparation of the brick samples). The free CaO that had not reacted with silicates reacted with water and later with CO₂ forming crystals of 4–5 µm. The development of rough surfaces suggests the rapid growth of these crystals [49]. In the same Fig. 1g we can see part of the former carbonate crystal which managed to react with silicates forming gehlenite on the edge of the pore with approximately equal amounts of Mg and Al. The pure gehlenite indicated by XRD analyses (Table 5) is not therefore being formed and instead what we see is an intermediate phase of the åkermanite-gehlenite series. This is because XRD is unable to correctly distinguish the end-members of this series [50].

3.2. Porous system

The addition of sawdust (in its varying percentages) had a greater effect on the hydric behaviour of the bricks than changes in the firing temperature. Fig. 2 clearly shows that when the amount of sawdust is increased, their water absorption capacity also increases. This is manifested in the free and forced water absorption values (A_b and A_f , Table 6), which are twice as high in the bricks with 10% added sawdust than in those made without additives. Increases in the firing temperature can affect the hydric behaviour of the brick samples in each group due to increasing vitrification as described above in the previous section (see Table 5 and Fig. 1). Indeed, at the beginning of the hydric test, the samples fired at 1100 °C absorbed water more slowly than the other samples, but by the time they reached forced saturation the bricks fired at 1100 °C had absorbed more water than those fired at 950 °C, which in turn had absorbed more than those fired at 800 °C (Fig. 2). These differences are a sign of the changes that the porous system undergoes as firing temperature increases. The capillaries between the pores become more tortuous making it more difficult for the bricks to absorb water. The tortuousness of the porous system is assessed by measuring the degree of interconnection between pores (A_x , Table 6) and comparing A_b and A_f . As the difference between these two values increases (the slope of the curve in Sector 2 of Fig. 2 increases) the communication between the pores becomes more difficult [31]. These values are closely related to firing temperature in that the highest values (i.e. poor interconnection) can be seen in the samples fired at the highest temperature.

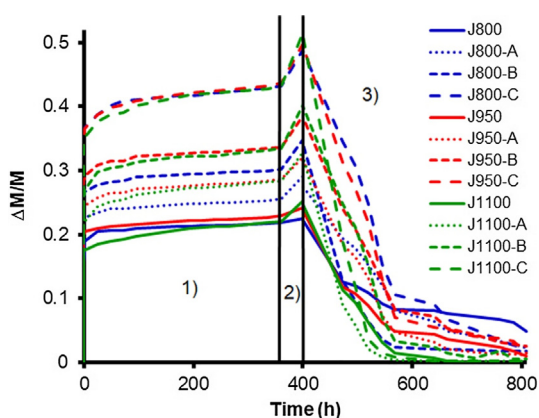


Fig. 2. Free water absorption (1), forced water absorption (2) and drying (3) of bricks made without additives and with the addition of sawdust. Weight variation ($\Delta M/M$) versus time (in h). Each curve represents the mean of three measurements. Brick abbreviations are indicated in Table 1.

The presence of sawdust makes these interconnections worse, above all when 5% and 10% of sawdust were added. A_x values are inversely proportional to the saturation coefficient (S , Table 6), in that the most highly saturated samples are those with the best connections between the pores. This is the case of J800 and J950 in which the saturation value is around 90%.

The speed at which a brick dries out is another useful parameter when it comes to assessing its durability, given that water is involved in most decay processes [33]. In this case, the drying index offers little help for comparison purposes in that all the studied bricks had similar values (D_i , Table 6). However, if one looks at the changing slopes in the drying curves (point 3 of Fig. 2), one can see that the drying process varies from one sample to the next. Curves show an initial straight slope or “constant drying rate” [51] in which the porous system of bricks does not affect the drying process. Drying occurs only by the diffusion of vapour from the wet surfaces of samples into the environment. This first stage is quite short in bricks fired at 800 °C and 950 °C, especially when sawdust is added. Drying takes longer, however, in samples fired at 1100 °C (see J1100-C, Fig. 2). The drying rate changes when “critical moisture content” [51] is reached and water begins to be lost due to its movement from the pores to the surface. This change in the slope of the curves is known as the “falling drying rate” [51], a phase of the drying process in which pore radii are very influential because the water moves towards the surface by capillarity [52]. The drying process in J800 (which still retains a significant amount of water at the end of test) and, in general, in those fired below 1100 °C is dominated by the falling drying rate. This seems to be due to the absence of the large rounded pores observed by ESEM which developed after the vitrification of the matrix at 1100 °C. As regards open porosity (P_o , Table 6), this increases in line with increasing concentrations of sawdust. Samples without additives absorb the least water and have the lowest P_o values of between 33 and 37%. These values are clearly higher than those usually found in industrially produced bricks manufactured by extrusion [53], but in line with the porosity of handmade bricks [54,55]. The bricks with 10% added sawdust absorb more water and have up to 60% porosity making them substantially lighter than normal bricks. In fact, apparent density (ρ_a , Table 6) falls from 1.5 g/cm³ in bricks without additives to 1 g/cm³ in bricks made with 10% of added sawdust. Bricks without additives have the lowest real density (ρ_r) values.

The mercury intrusion porosimetry (MIP) technique confirms the influence of sawdust on changes in the porous system of the bricks and on the pore size range. Indeed if one compares the porosimetric curves of bricks made without additives to those made with added sawdust, the former have a clearly unimodal distribution (Fig. 3) with a maximum peak that shifts towards larger pore sizes as the firing temperature increases (from 0.25 µm at 800 °C to 0.53 µm at 950 °C and 0.75 µm at 1100 °C). The latter by contrast are bimodal. Sawdust is responsible for the formation of a second group of pores at around 10 µm, and this group increases in size in line with the sawdust content. These pores appeared after the disappearance of the sawdust fibres which were burnt during firing of the bricks and which were earlier observed using ESEM (Fig. 1). Also in the bricks made with added sawdust peaks for both families of pores shift towards higher pore sizes between 800 and 1100 °C. The displacement of the pores and their dependence on the firing temperature or the sawdust content can be better understood after the analysis of pore sizes at different ranges in Table 6. In fact, the number of pores with radii of over 1 µm increases in all the bricks in line with increasing sawdust content, while the number of pores between 0.1 and 1 µm falls (Table 6). The family of pores comprised between 0.01 and 0.1 µm are the most influenced by the firing temperature in that they are only affected by the sawdust content in poorly vitrified

Table 6

Results of hydric and MIP tests on brick samples made without additives and with added sawdust. The standard deviation for each result of the hydric tests is indicated in brackets. A_b = free water absorption (%); A_f = forced water absorption (%); A_x = degree of pore interconnection; Di = drying index; S = saturation coefficient (%); P_o and P_{oMIP} = open porosity (%), the second determined by MIP); ρ_a and ρ_{aMIP} = apparent density ($g\ cm^{-3}$, the second determined by MIP); ρ_r and ρ_{rMIP} = real density ($g\ cm^{-3}$, the second determined by MIP); SSA = specific surface area (m^2/g , determined by MIP); >1 = percentage of pores higher than $1\ \mu m$; $0.1-1$ = percentage of pores comprised between $0.1\ \mu m$ and $1\ \mu m$; $0.01-0.1$ = percentage of pores comprised between $0.01\ \mu m$ and $0.1\ \mu m$; <0.01 = percentage of pores lower than $0.01\ \mu m$ (all determined by MIP). Brick abbreviations are indicated in Table 1.

	J800	J800-A	J800-B	J800-C	J950	J950-A	J950-B	J950-C	J1100	J1100-A	J1100-B	J1100-C
A_b	21.82 (0.47)	25.54 (1.35)	30.17 (0.15)	43.20 (1.16)	22.94 (0.78)	28.76 (0.65)	33.56 (1.26)	43.66 (1.15)	22.06 (0.49)	28.39 (0.01)	33.50 (0.13)	43.30 (0.11)
A_f	22.31 (0.06)	27.83 (4.16)	34.53 (0.95)	48.48 (2.27)	23.79 (1.15)	31.78 (0.64)	38.39 (1.16)	49.46 (0.17)	24.50 (0.01)	32.50 (0.06)	39.67 (0.51)	51.03 (0.49)
A_x	2.21 (1.83)	7.56 (8.97)	12.59 (1.95)	10.85 (1.77)	3.55 (1.41)	9.50 (0.20)	12.58 (0.63)	11.72 (2.63)	9.94 (1.96)	12.66 (0.12)	15.56 (1.40)	15.13 (1.03)
Di	0.90 (2.54)	0.88 (8.22)	0.83 (3.84)	0.83 (1.33)	0.88 (2.37)	0.85 (2.70)	0.85 (0.94)	0.82 (1.18)	0.86 (2.48)	0.83 (2.39)	0.83 (0.74)	0.78 (0.00)
S	92.42 (0.14)	86.81 (3.53)	81.91 (1.18)	82.62 (11.12)	89.66 (1.24)	83.44 (0.80)	81.86 (1.79)	80.53 (2.62)	77.52 (0.24)	77.43 (0.35)	76.49 (0.40)	76.03 (0.37)
P_o	33.88 (0.01)	39.51 (0.09)	45.74 (0.00)	60.90 (0.17)	35.95 (0.02)	43.76 (0.00)	49.62 (0.01)	53.81 (0.05)	37.19 (0.01)	45.21 (0.01)	50.25 (0.01)	57.52 (0.02)
ρ_a	1.52 (0.02)	1.43 (0.00)	1.32 (0.05)	1.25 (1.41)	1.51 (0.01)	1.38 (0.03)	1.29 (0.11)	1.09 (0.24)	1.52 (0.03)	1.39 (0.03)	1.27 (0.01)	1.13 (0.07)
ρ_r	2.30 (0.04)	2.36 (0.00)	2.44 (0.01)	3.40 (0.02)	2.36 (0.03)	2.45 (0.00)	2.57 (0.02)	2.36 (0.01)	2.42 (0.01)	2.54 (0.01)	2.55 (0.01)	2.65 (0.00)
SSA	7.96	11.92	11.29	10.71	6.34	6.28	5.85	5.74	2.06	1.35	4.94	4.67
P_{oMIP}	38.45	41.13	45.93	55.46	42.79	47.66	49.08	58.58	43.29	46.58	52.88	59.62
ρ_{aMIP}	1.61	1.56	1.45	1.19	1.58	1.44	1.41	1.13	1.56	1.49	1.31	1.12
ρ_{rMIP}	2.61	2.65	2.67	2.68	2.77	2.75	2.76	2.73	2.76	2.80	2.78	2.77
>1	3.69	14.73	24.34	48.35	2.04	15.02	27.58	43.71	7.52	22.57	35.58	50.86
$0.1-1$	66.5	56.1	51.58	35.17	88.1	74.41	62.5	47.55	91.21	75.92	60.75	46.52
$0.01-0.1$	28.85	26.7	22.41	14.97	8.04	9.81	8.98	8.41	0.98	1.51	2.95	2.12
<0.01	0.96	2.46	1.77	1.51	1.82	0.76	0.95	0.33	0.29	0	0.72	0.49

bricks, i.e. those fired at $800\ ^\circ C$, in which there is a fall in the number of these pores as the sawdust content increases. In the samples fired at $950\ ^\circ C$ and over there is a dramatic decrease in the number of these pores, above all at $1100\ ^\circ C$, and no variations due to sawdust content can be observed. The porosity of the bricks is increased by the addition of sawdust, and this porosity increases in line with the percentage of sawdust and also with increases in the firing temperature (P_{oMIP} , Table 6), so confirming the results of the hydric tests. It is interesting to observe how the specific surface area (SSA , Table 6) falls as the firing temperature rises. This is due to the gradual disappearance of the smallest pores of less than $0.01\ \mu m$. These can be found in bricks fired at $800\ ^\circ C$ (Fig. 3) and gradually come together forming larger pores as the temperature increases. Indeed, in a similar way to the family of pores ranging between 0.01 and $0.1\ \mu m$, the percentage of pores of less than $0.01\ \mu m$ is lower at $950\ ^\circ C$ and very scarce at $1100\ ^\circ C$ (Table 6) because of the vitrification of the bricks. This explains why different slopes were observed in the drying curves in the hydric tests (Fig. 2). Apparent density values (ρ_{aMIP} , Table 6) fell in line with an increase in sawdust content, as was observed in the hydric tests. Similar changes do not occur in real density (ρ_{rMIP} , Table 6) as this depends on the mineralogy rather than on the porous system and increases, albeit only slightly, in line with increasing firing temperature due to the higher density of the newly-formed minerals (gehlenite, anorthite, diopside and wollastonite) compared to those which disappeared or whose concentrations fell (quartz, illite/muscovite and calcite) (Table 5).

3.3. Compactness

Analysing the values in Table 7, V_{p1} is always the lowest velocity compared to V_{p2} and V_{p3} because in V_{p1} the waves are propagated perpendicular to the orientation of phyllosilicates and of the elongated pores that took the place of the sawdust fibres that were burnt during firing. This preferential orientation took place during the preparation of unfired pieces when the clayey mass

was compacted into the mould. Both the firing temperature and the addition of sawdust influenced ultrasound velocity: the velocity increased when firing temperature increased and fell in line with increases in sawdust content. In the case of firing temperature, the vitrification of samples and the generation of new mineral phases (gehlenite, anorthite, diopside and wollastonite, Table 5) gave rise to a more compact structure, so favouring quicker transmission of the waves. The addition of sawdust, as expected, reduces the P-wave velocity because it increases the empty spaces. Indeed, the bricks that propagated the waves more quickly are those made without additives and in particular those fired at $1100\ ^\circ C$, which reach an average velocity of $2440\ m/s$ (Table 7). When sawdust was added, the velocity fell and the higher the sawdust content, the more it fell. Indeed, the lowest V_p values were reached with 10% sawdust content and a firing temperature of $800\ ^\circ C$ ($1662\ m/s$, Table 7). Another interesting fact is that compactness did not increase gradually with the increase in temperature. In fact, between $800\ ^\circ C$ and $950\ ^\circ C$ there was little difference between the velocity values as compared to the sharp rise that took place between $950\ ^\circ C$ and $1100\ ^\circ C$. This means that bricks do not reach a high degree of sintering and vitrification of the matrix until $1100\ ^\circ C$, making them very compact. As regards anisotropy values, absolute anisotropy behaves more consistently than relative anisotropy. This is because absolute anisotropy considers the velocity in three directions of space that are mutually perpendicular, while relative anisotropy only takes two directions into account (those lying parallel to the orientation of phyllosilicates). This means that relative anisotropy values may be altered during the preparation of unfired samples when they are cut into cubes with cotton thread, in that as the thread cuts through the sample, it can change the orientation of the laminar minerals. As the firing temperature increases, bricks become more isotropic due to an increase in vitrification and ΔM falls. It is interesting to note that the addition of sawdust makes bricks more anisotropic due to the preferential orientation of the elongated pores generated by the organic fibres.

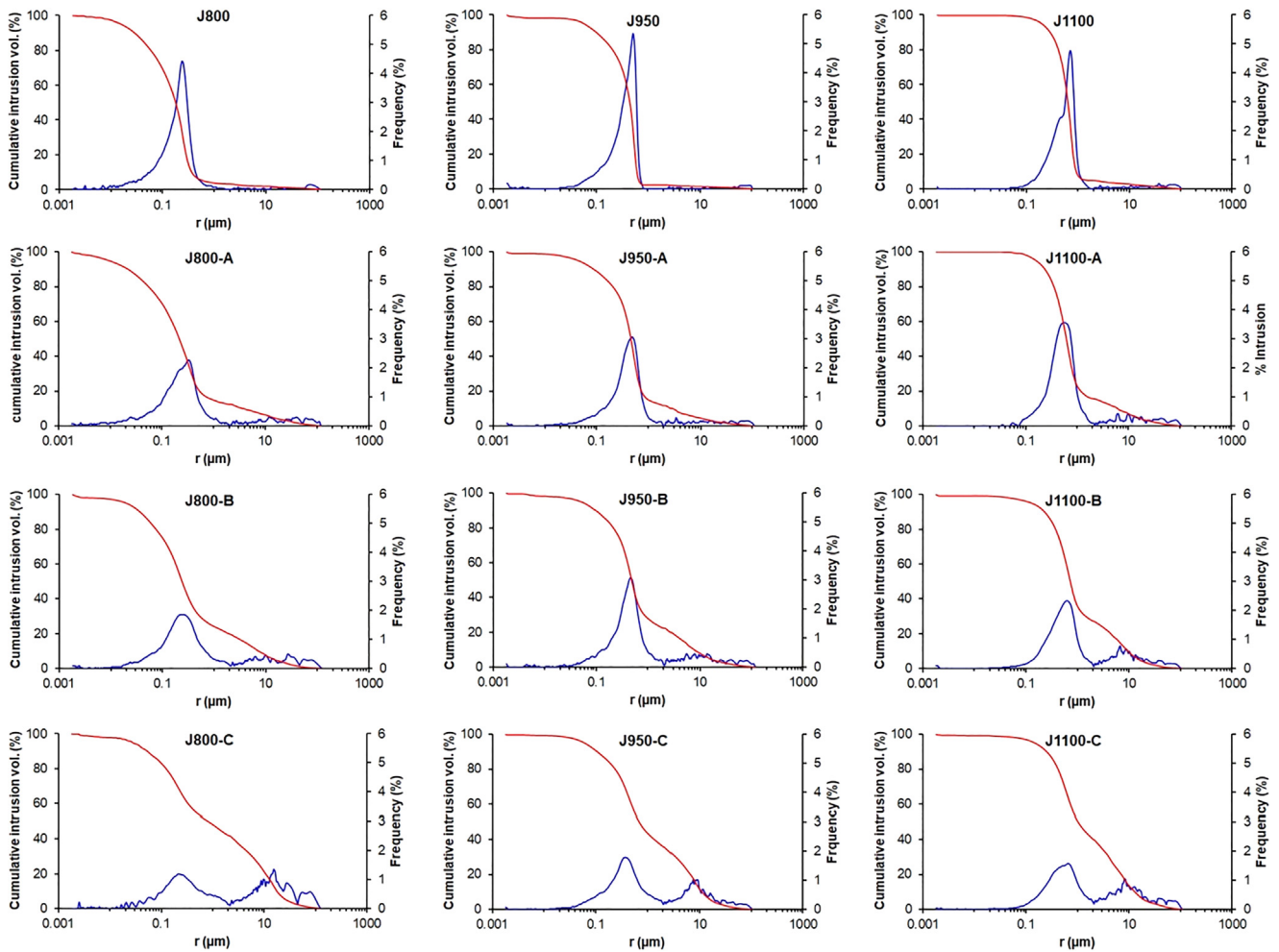


Fig. 3. Cumulative mercury intrusion (red) and pore size distribution (blue) curves of bricks made with and without added sawdust. Brick abbreviations are indicated in Table 1. (For interpretation of the references to colour in this figure legend, the reader is referred to the web version of this article.)

Table 7
Speed of ultrasonic wave propagation in the three orthogonal directions (V_p , in m/s), mean velocity (\bar{V}_p , in m/s), structural (ΔM), and relative (Δm) anisotropies (in %) of bricks made with and without sawdust. The standard deviation is indicated in brackets. V_{p1} , V_{p2} , and V_{p3} are the ultrasound velocities measured in three orthogonal directions. Brick abbreviations are indicated in Table 1.

	V_{p1}	V_{p2}	V_{p3}	\bar{V}_p	ΔM	Δm
J800	1793 (5.89)	2105 (19.54)	2216 (8.06)	2038	17.01	5.14
J800-A	1706 (14.88)	2187 (6.98)	2252 (6.14)	2048	23.14	2.93
J800-B	1507 (12.97)	2057 (12.82)	2092 (7.16)	1885	27.36	1.69
J800-C	1332 (23.26)	1796 (16.31)	1859 (14.72)	1662	27.11	3.45
J950	2202 (23.52)	2230 (25.23)	2405 (11.32)	2279	4.98	7.55
J950-A	1827 (11.13)	2144 (9.77)	2242 (27.16)	2071	16.69	4.47
J950-B	1589 (6.61)	2068 (13.95)	2069 (6.54)	1909	23.18	0.05
J950-C	1336 (15.01)	1824 (14.38)	1878 (11.80)	1679	27.82	2.92
J1100	2291 (21.26)	2497 (24.37)	2533 (10.29)	2440	8.91	1.43
J1100-A	2126 (41.15)	2254 (19.95)	2440 (14.70)	2273	9.42	7.93
J1100-B	1886 (15.50)	2287 (8.89)	2352 (5.92)	2175	18.69	2.80
J1100-C	1562 (4.10)	1761 (6.28)	2095 (8.76)	1806	18.98	17.32

A comparative analysis of detailed parameters determined by hydric tests, MIP and ultrasound was conducted to provide more information about the influence of the firing temperature and the amount of sawdust on the behaviour of bricks. Fig. 4a compares the mean ultrasonic velocity (\bar{V}_p) with the apparent density (ρ_{aMIP}) highlighting a direct relationship between these two values. As one might expect, velocity increases as the bricks get denser. This behaviour is clearly related to the amount of sawdust: the lower the sawdust content, the lower the porosity,

so increasing the compactness of the bricks and therefore the ultrasonic velocity. The values in the diagram were enclosed in four different dotted areas depending on the amount of sawdust (0%, 2.5%, 5% and 10%). The position of each sample is closely related to the firing temperature: the bricks fired at 1100 °C are all on the right-hand side of each area while those fired at 800 °C are on the left because the increase in firing temperature results in higher vitrification and therefore in higher compactness and density of the bricks.

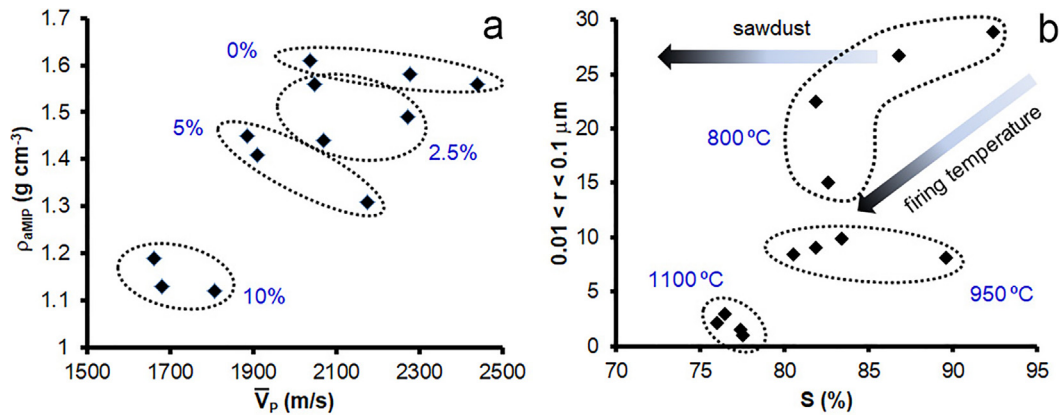


Fig. 4. Comparison of detailed parameters to observe the influence on brick samples of firing temperature and sawdust content: a = mean velocity (\bar{V}_p , in m/s) versus apparent density (ρ_{AMIP} , in g cm⁻³); b = saturation coefficient (S, in %) versus pore radii range between 0.01 and 0.1 μm . Dotted areas enclose samples with different sawdust content (figure a) and different firing temperatures (Figure b).

Fig. 4b compares the saturation coefficient (S) and the pore size ranging between 0.01 and 0.1 μm . At first glance, it seems that the samples are scattered in the diagram. However, when the firing temperature information is added (samples fired at the same temperature were enclosed in dotted areas), the diagram reveals that the saturation coefficient falls as the firing temperature and sawdust content increase. Moreover, the increase in the firing temperature considerably reduces the number of small pores. As mentioned in FESEM and MIP observations, the coalescence of pores and the development of a “cellular structure” due to the vitrification of the matrix reduce the number of small pores. It is interesting to note that the bricks are more highly dispersed at low firing temperatures. High firing temperatures produce very similar samples in terms of their saturation capacity, while a lower degree of vitrification increases the distance between the values.

3.4. Colour

Fig. 5 shows the varying colour and general appearance of the bricks. Samples are generally red-yellow coloured but there are certain differences between them that have been quantified by spectrophotometry. When comparing lightness results (L^* , Fig. 6a) two different forms of behaviour can be observed. When sawdust is not present or only in low concentrations (samples J and J-A), bricks become lighter in colour when the firing temperature increases. However, in those with higher sawdust content (5% and 10%) the opposite occurs: samples J-B and J-C are lighter in colour especially at the highest firing temperature. These differences are more obvious when the two most extreme groups of bricks are compared, those made without additives (J) and those made with 10% added sawdust (J-C). Research has shown that compositional and textural variations can alter the chromatic parameters of materials [56]. In our case the differences in lightness results must be due to the number of pores, which varies according to the percentage of sawdust and the degree of vitrification of the bricks. Changes in mineralogy may also be a factor. It is logical to imagine that vitrification will modify the surface of the samples making them smoother and more uniform. This change increases the lightness of the bricks made without additives or with just a small amount of sawdust. Higher sawdust content makes the bricks (and their surfaces) more porous (see P_o and P_{oMIP} values, Table 6) and it is possible that partially reducing conditions may have been established in the kiln during firing [57], leading to a fall in L^* , above all at 1100 °C. Indeed, bearing in mind the slightly darker appearance of these bricks, it is possible that maghemite (Fe_2^3+O_3) has crystallized. However, the fact that the reflections of

this oxide overlap with other mineral phases present in the bricks prevented us from identifying it unequivocally using XRD. There was also no decrease in the quantity of hematite, the mineral responsible for the red pigmentation of bricks, as the sawdust content increased (Table 5). According to De Bonis et al. [58], the darkening of bricks may be due to an increase in the size of hematite crystals scattered throughout the matrix.

Chromaticity (a^* and b^* , Fig. 6b) results also highlight the differences between the materials on the basis of composition and firing temperature. These differences are due essentially to parameter a^* (in which positive values indicate the amount of red), which varies between 5 and 17, rather than to parameter b^* , which maintains an almost constant yellow value of between 20 and 22. More detailed analysis of these results shows that the bricks fired at 1100 °C had the lowest a^* values, which means that the red component of colour is less intense. As firing temperature falls, a^* values increase and this increase is also associated with the composition of bricks in that a^* increases when sawdust content falls. The bricks with the most intense colour (most saturated) are those made without additives.

The colour difference between bricks made without additive and those with added sawdust (ΔE , Table 8) remains below 6.3 and no clearly defined pattern can be observed. According to Grossi et al. [59], chromatic changes of more than 5 can be observed by the human eye. This means that in some cases, above all sample J1100-C, it may be possible to distinguish the change in colour.

3.5. Thermal conductivity

IR thermography was used to qualitatively compare the degree of thermal refractoriness of the bricks. The height reached by the isotherms in samples that were heated for 30 min at 50 °C was measured. This test showed that within each group of bricks (i.e., without additive and with 2.5%, 5% and 10% of sawdust content), heat was propagated more quickly as firing temperature increased. Lassinantti Gualtieri et al. [60], Saiah et al. [61] and Šveda et al. [62] observed that the thermal conductivity of a ceramic material is influenced by numerous factors. These include its mineralogical composition, moisture content, the grain size of the raw material and above all the apparent density, porosity and pore size distribution, with the least dense, most porous samples being found to be the most refractory. This means that the data obtained in this research appears to contradict that set out in the bibliography given that in each group the bricks that transmitted most heat were the most porous ones (see P_o and P_{oMIP} values Table 6). On this question it is important to remember that the increase in

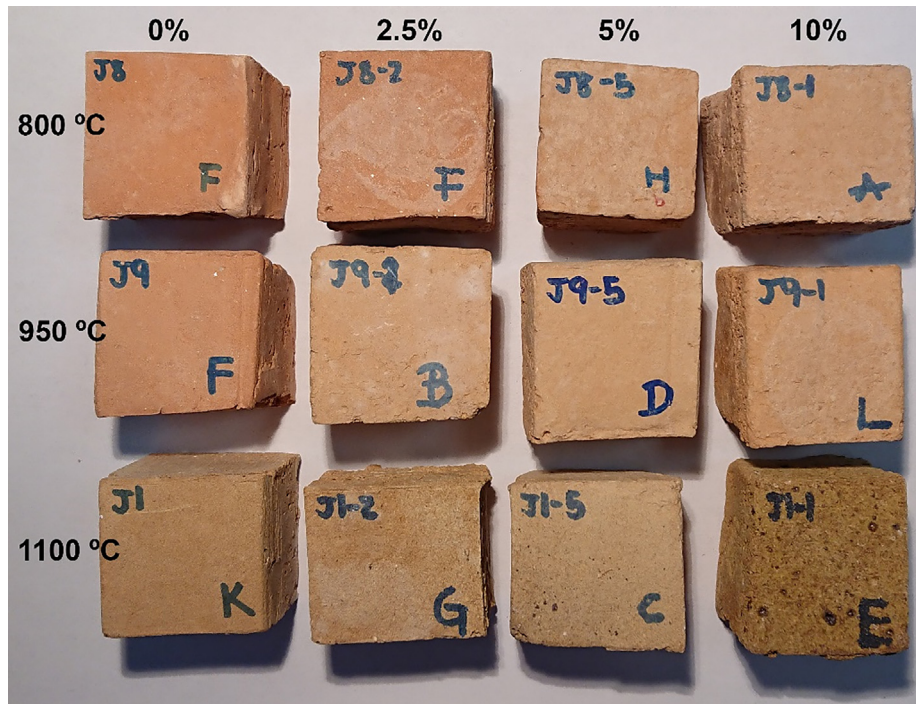


Fig. 5. Colour of fired bricks without the addition of sawdust (0%) and with added 2.5%, 5% and 10% sawdust fired at 800, 950 and 1100 °C. Brick cubes have a 4 cm-edge.

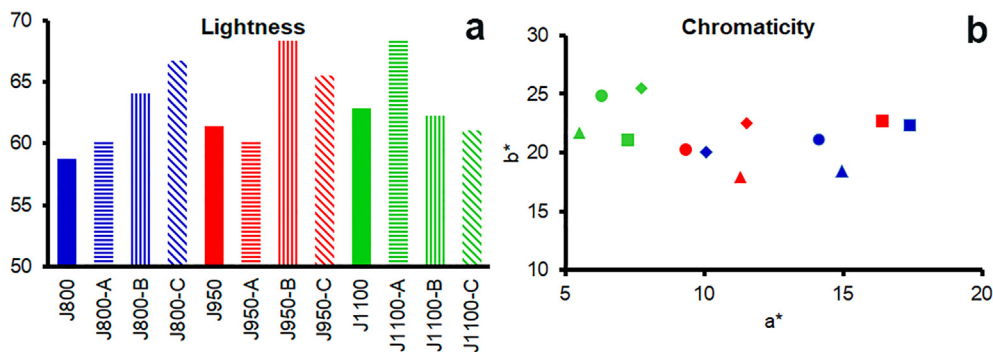


Fig. 6. Lightness (a) and chromaticity (b) of bricks. Blue stands for bricks fired at 800 °C; red for bricks fired at 950 °C; green for bricks fired at 1100 °C; the squares represent bricks without sawdust; the triangles represent those with added 2.5 wt% sawdust; the circles represent those with added 5 wt% sawdust; the diamonds represent those with added 10 wt% sawdust. Brick abbreviations are indicated in Table 1. (For interpretation of the references to colour in this figure legend, the reader is referred to the web version of this article.)

Table 8
Colour difference (ΔE) caused by the addition of sawdust to the bricks with respect to those made without additive. Standard deviation (σ) is also indicated. Brick abbreviations are indicated in Table 1.

	J800-A	J800-B	J800-C	J950-A	J950-B	J950-C	J1100-A	J1100-B	J1100-C
ΔE	5.90	5.97	3.41	5.91	4.11	4.62	5.63	4.01	6.31
σ	1.29	2.43	0.64	1.74	1.59	1.10	0.60	0.92	2.54

temperature gave rise to samples with a higher degree of vitrification and a stronger bond between the particles, above all at 1100 °C, which made them more compact (a/c values in Table 5 and V_p values in Table 7). This suggests that the stronger bond between the components of the brick is more influential than the increase in porosity in the transmission of heat. In addition, when bricks with different composition but fired at the same temperature are compared, an increase in their refractoriness can be observed in line with increasing sawdust content. Fig. 7 shows the transmission of heat in bricks made without additive and those

made with 10% in weight of sawdust fired at 800 °C and 1100 °C (samples J800, J800C, J1100 and J1100-C, respectively). The propagation of heat is more difficult in samples made with sawdust, in other words in the most porous samples. IR images also show that from the beginning of the test the transmission of heat was not uniform in the samples made with sawdust, which after just a few minutes makes it difficult to measure the height reached by the heat (Fig. 7a and c). At the beginning of the test the bricks made with added sawdust seemed to transmit heat at the same velocity as the bricks made without additives (Fig. 7a) or more quickly

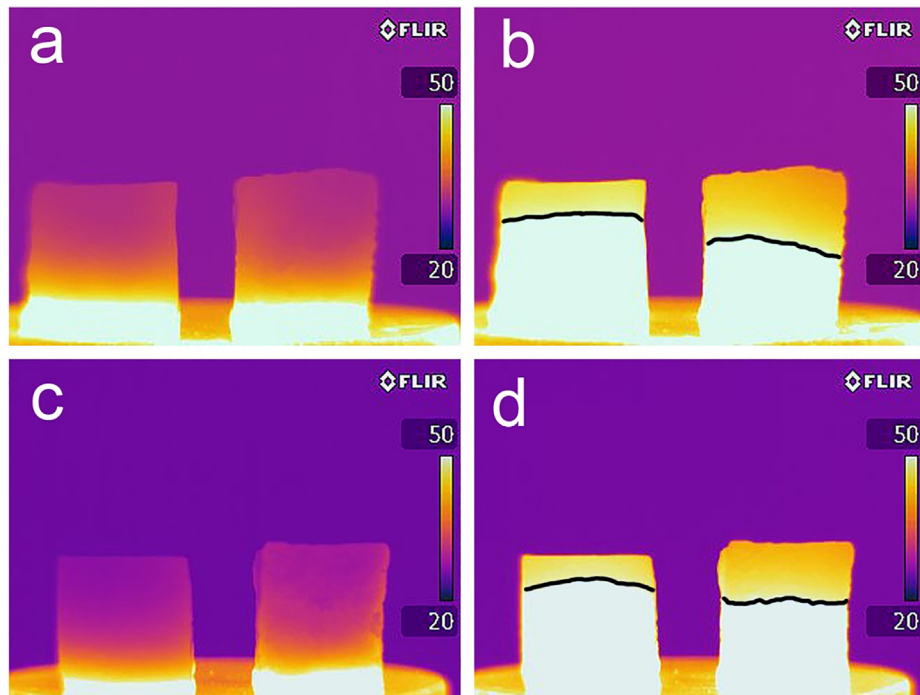


Fig. 7. Representative IR thermographic images showing bricks made without additives (on the left of each image) and with 10 wt% of sawdust (on the right of each image) fired at 800 °C (images a and b) and at 1100 °C (images c and d). Images were taken after 2 min (a and c) and 30 min of heating (b and d). The continuous lines in images b and d mark the 50 °C isotherm. The height of the samples varies from 3.9 cm to 4.1 cm.

(Fig. 7c). However, as time went by, the bricks made with sawdust found it more difficult to propagate the heat and half an hour into the test, the isotherm marking 50 °C had not reached the same height as in the bricks made without additives. A certain degree of irregularity in the isotherm could be observed in the presence of high porosity (Fig. 7b and d). It is interesting to note that the difference in the height of the isotherms of bricks was more accentuated at 800 °C than at 1100 °C. This is due once again to the high degree of vitrification reached by the bricks fired at 1100 °C, which favours more rapid transmission of heat, so much so that there are only slight differences between the samples made with and without additives (Fig. 7d).

3.6. Salt crystallization test

The accelerated ageing test revealed that within each group of bricks, the samples that increased least in weight as a result of the crystallisation of sodium sulphate inside them were those fired at 1100 °C. While the bricks that gained most weight and suffered the greatest weight variations were those fired at the lowest temperature (Fig. 8). With the naked eye, it is possible to observe that fragments have been lost, generally along the edges of the sample. This fragment loss is normally higher, the higher the sawdust content of the brick and the lower the firing temperature.

If one looks at the bricks in more detail, at 800 °C (blue curves, Fig. 8) the brick with least fluctuations in weight was the one made without additives (J800). The weight of this material increases until cycle 11 after which it undergoes a slight decline in cycle 12. The salts which had crystallized inside it up until that point crack the brick causing fragments to fall off (with the resulting weight loss). From cycle 13 onwards, the weight of J800 rises again due to the presence of salts in new fissures. If we observe the behaviour of the other samples fired at 800 °C, variations in weight are more pronounced and start happening earlier (cycle 5). More

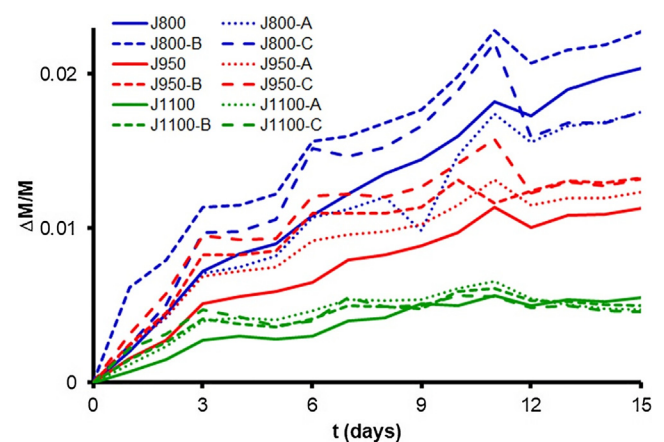


Fig. 8. Weight variation in bricks made without additives and with added sawdust during 15 salt crystallization test cycles. Each cycle corresponds to 1 day and each curve represents the mean of three measurements. Brick abbreviations are indicated in Table 1.

substantial weight losses are also observed, such as for example in cycle 9 in J800-A or cycle 12 in J800-C (Fig. 8).

When the firing temperature is increased to 950 °C, the bricks become more resistant to salt crystallization and their weight increases less over the 15 cycles. These samples follow a similar pattern to those fired at 800 °C, in other words those with the highest sawdust content experience the greatest variations in weight (red curves, Fig. 8).

At 1100 °C the differences between the types of bricks are much less noticeable and in some places the curves even overlap slightly (green, Fig. 8). This indicates that the degree of vitrification of these bricks is more influential in the damage they suffer when subject to salt attack than the amount of additive. In other words, at this temperature the porosity developed by the addition of sawdust is less

significant than the strength reached by the highly vitrified matrix of the bricks. Elert et al. [63] and Benavente et al. [64] observed that salt crystallization affects the samples with small pores (below 1 μm) more than those with large rounded ones. This seems to contradict the evidence in Fig. 8 where the samples with larger pores (see porometric curves, Fig. 3) showed higher mass increments and more significant mass fluctuations (mainly at 800 and 950 °C). The higher mass increment is due to the higher porosity of the bricks made with sawdust, which allows greater absorption of saline solution. For its part, the greater fluctuation in mass is due to the fact that the larger pores can act as a reservoir for water and salts that feeds the smaller pores and causes extensive material loss. In this case, the damage suffered by the bricks depends on the way the saline solution is transported and propagated through the pore network [65,66]. In addition, the more porous the material is, the more vulnerable it is to decay due to the weaker union between the particles [33]. This is why mass increment and fluctuation appear low at 1100 °C thanks to the high degree of vitrification of the bricks fired at this temperature (see ESEM observation, Fig. 1). This creates a stronger union between the grains and a more compact structure, so limiting the impact of salt crystallization.

4. Conclusions

In this paper the effects of the addition of a waste product, beechwood sawdust, on the quality of solid bricks was assessed from mineralogical, textural and physical points of view, comparing the results obtained by these bricks with those obtained by other identical bricks made with exactly the same raw material (from Jun, Granada), preparation process (manual) and firing temperatures (between 800 °C and 1100 °C), but with no additives. The following conclusions were reached:

1. The mineralogical changes that take place during the brick firing process are a direct result of the composition of the raw material, which is rich in silicates and carbonates. The amount of quartz, the most abundant mineral phase in the raw material, falls because it reacts with carbonates to form new mineral phases. The amount of phyllosilicates also falls to the point of disappearing above 950 °C. Gehlenite, anorthite, diopside and wollastonite appear as the firing temperature increases. The quantity of amorphous phase also rises due to the vitrification of the bricks.
2. Hematite is responsible for the red–yellowy colour of the bricks even though it is only present in small quantities. As the firing temperature of the bricks increases, so chromaticity component a^* falls.
3. The addition of sawdust does not cause significant changes in the colour of the bricks or in their mineralogy, nor does it increase the amount of amorphous phase in the fired samples. Similarly, no evidence was found to suggest that the combustion of organic matter induced a reduction atmosphere inside the kiln.
4. The addition of sawdust causes significant changes in the porous system, in which it creates a new family of pores, reaching almost 60% of porosity when 10% in weight of sawdust was used as an additive, as compared to 38% porosity in bricks made without additives. The bricks become lighter and the apparent density falls to 1 g/cm^3 .
5. The addition of sawdust makes the bricks more susceptible to deterioration. The formation of larger pores creates reservoirs of saline solution, which is transported around the porous system causing the bricks to decay.
6. The bricks with a 10% sawdust content fired at 800 °C are the least resistant to salt crystallization. This is because of the weak union between the grains in a poorly vitrified matrix.
7. The increase in firing temperature improves the physical properties of the bricks, above all at 1100 °C when there is evidence of widespread vitrification in the texture. This gives rise to more compact, less anisotropic bricks, although they transmit heat more quickly, suggesting poorer insulation properties.
8. By contrast the bricks fired at 800 °C perform better as regards thermal insulation, which also increases with the addition of sawdust, above all with 10% in weight, due to the increased porosity of the bricks.

In general, certain physical properties such as compactness and resistance to salt crystallization were better in bricks made without additives and fired at 1100 °C. However, the addition of sawdust did not change the mineralogy of bricks and had certain advantages. It made the bricks lighter and better thermal insulators, for which extensive vitrification was not required. This would enable them to be fired at lower temperatures, so reducing energy costs. This research has demonstrated that high firing temperatures do not improve the insulating properties of bricks. Future research must consider the mechanical behaviour of bricks made with sawdust in order to assess their suitability as a building material.

Declaration of Competing Interest

The authors declare that they have no known competing financial interests or personal relationships that could have appeared to influence the work reported in this paper.

Acknowledgments

This study was funded by Junta de Andalucía Research Group RNM179 and by the Research Project MAT2016-75889-R. We thank Cerámica Castillo Siles for providing the raw material used to prepare and fire the bricks. We are grateful to Nigel Walkington for his assistance in translating the original text.

References

- [1] Y. Taha, M. Benzaazoua, R. Hakkou, M. Mansori, Coal mine wastes recycling for coal recovery and eco-friendly bricks production, *Miner. Eng.* 107 (2017) 123–138.
- [2] D. Eliche Quesada, L. Leite Costa, Use of bottom ash from olive pomace combustion in the production of eco-friendly fired clay bricks, *Waste Manage.* 48 (2016) 323–333.
- [3] P. Muñoz Velasco, M.P. Morales Ortiz, M.A. Mendivil Giro, M.C. Juárez Castelló, L. Muñoz Velasco, Development of better insulation bricks by adding mushroom compost wastes, *Energy Build.* 80 (2014) 17–22.
- [4] S.M.S. Kazmi, M.J. Munir, I. Patnaikuni, Y.F. Wu, U. Fawad, Thermal performance enhancement of eco-friendly bricks incorporating agro-wastes, *Energy Build.* 158 (2018) 1117–1129.
- [5] A. Al Fakih, B.S. Mohammed, M. Shahir Liew, E. Nikbakht, Incorporation of waste materials in the manufacture of masonry bricks: an update review, *J. Build. Eng.* 21 (2019) 37–54.
- [6] C. Bories, M.E. Borredon, E. Vedrenne, G. Vilarem, Development of eco-friendly porous fired clay bricks using pore-forming agents: a review, *J. Environ. Manage.* 143 (2014) 186–196.
- [7] S.N. Monteiro, C.M. Fontes Vieira, On the production of fired clay bricks from waste materials: a critical update, *Constr. Build. Mater.* 68 (2014) 599–610.
- [8] Z. Zhang, Y.C. Wong, A. Arulrajah, S. Horpibulsuk, A review of studies on bricks using alternative materials and approaches, *Constr. Build. Mater.* 188 (2018) 1101–1118.
- [9] B. Chemani, H. Chemani, Effect of adding sawdust on mechanical-physical properties of ceramic bricks to obtain lightweight building material, *Int. J. Mech. Mechatr. Eng.* 6 (2012) 2521–2525.
- [10] M.M. Esperanza Quintana, Combustión y pirólisis de residuos orgánicos: análisis de contaminantes PhD Thesis, University of Alicante, Spain, 2000.
- [11] D. Eliche Quesada, M.A. Felipe Sesé, J.A. López Pérez, A. Infantes Molina, Characterization and evaluation of rice husk ash and Wood ash in sustainable clay matrix bricks, *Ceram. Int.* 43 (2017) 463–475.
- [12] D. Eliche Quesada, F.A. Corpas Iglesias, L. Pérez Villarejo, F.J. Iglesias Godino, Recycling of sawdust, spent earth from oil filtration, compost and marble residues for brick manufacturing, *Constr. Build. Mater.* 34 (2012) 275–284.

- [13] O. Benjeddou, C. Soussi, M.A. Khadimallah, R. Alyousef, M. Jedidi, Development of new baked bricks based on clay and sawdust 01040, in: *MATEC Web Conf.*, 2018, pp. 1–8.
- [14] I. Demir, Effect of organic residues addition on the technological properties of clay bricks, *Waste Manage.* 28 (2008) 622–627.
- [15] M. Arsenović, Z. Radojević, Ž. Jakšić, L. Pezo, Mathematical approach to application of industrial wastes in clay brick production – part II: optimization, *Ceram. Int.* 41 (2015) 4890–4898.
- [16] M. Arsenović, Z. Radojević, Ž. Jakšić, L. Pezo, Mathematical approach to application of industrial wastes in clay brick production – part I: testing and analysis, *Ceram. Int.* 41 (2015) 4899–4905.
- [17] B. Sena da Fonseca, A. Vilão, C. Galhano, J.A.R. Simão, Reusing coffee waste in manufacture of ceramics for construction, *Adv. Appl. Ceram.* 113 (2014) 159–166.
- [18] P. Muñoz Velasco, M.A. Mendivil, M.P. Morales, L. Muñoz, Eco-fired clay bricks made by adding spent coffee grounds: a sustainable way to improve buildings insulation, *Mater. Struct.* 49 (2016) 641–650.
- [19] S. Ozturk, M. Sutcu, E. Erdogmus, O. Gencil, Influence of tea waste concentration in the physical, mechanical and thermal properties of brick clay mixtures, *Constr. Build. Mater.* 217 (2019) 592–599.
- [20] I. González, E. Galán, A. Miras, M.A. Vázquez, CO₂ emissions derived from raw materials used in brick factories. Applications to Andalusia (Southern Spain), *Appl. Clay Sci.* 25 (2011) 193–198.
- [21] E. Lupiani Moreno, J. Soria Mingorance, Memoria de la Hoja n. 1009 (Granada). Mapa Geológico de España 1:50000, Instituto Geológico Minero de España, Servicio de Publicaciones, Ministerio de Industria y Energía, 1988, 73 pp.
- [22] D. Bajare, V. Svinka, Restoration of the historical brick masonry Venice, in: V. Fassina (Ed.), *Proceedings of the 9th International Congress on Deterioration and Conservation of Stone*, 2000, pp. 3–11.
- [23] F.C. Trevelyan, R.A. Haslam, Musculoskeletal disorders in a handmade brick manufacturing plant, *Int. J. Ind. Ergonom.* 27 (2001) 43–55.
- [24] G. Cultrone, C. Rodriguez Navarro, E. Sebastián, O. Cazalla, M.J. de la Torre, Carbonate and silicate phase reaction during ceramic firing, *Eur. J. Mineral.* 13 (2001) 621–634.
- [25] C. Rodriguez Navarro, E. Ruiz Agudo, A. Luque, A.B. Rodriguez Navarro, M. Ortega Huertas, Thermal decomposition of calcite: mechanisms of formation and textural evolution of CaO nanocrystals, *Am. Mineral.* 94 (2009) 578–593.
- [26] R.T. Laird, M. Worcester, The inhibiting of lime blowing, *Trans. Brit. Ceram. Soc.* 55 (1956) 545–563.
- [27] J.D. Martin, X Powder, X Powder 12, X Powder XTM. A software package for powder X-ray diffraction analysis, Lgl. Dp. GR-780-2016, 2016.
- [28] A.E. Charola, E. Wendler, An overview of the water-porous building materials interactions, *Restor. Build. Monum.* 21 (2015) 55–65.
- [29] UNE-EN 13755, Métodos de ensayo para piedra natural. Determinación de la absorción de agua a presión atmosférica, AENOR, Madrid, Spain, 2008.
- [30] NORMAL 29/88, Misura dell'indice di asciugamento (drying index), ICR-CNR, Rome, Italy, 1988.
- [31] G. Cultrone, M.J. de la Torre, E. Sebastián, O. Cazalla, Evaluación de la durabilidad de ladrillos mediante técnicas destructivas (TD) y no-destructivas (TND), *Mater. Construc.* 53 (2003) 41–59.
- [32] RILEM, Recommended test to measure the deterioration of stone and to assess the differences of treatment methods, *Mater. Struct.* 13 (1980) 175–253.
- [33] R.M. Esbert, J. Ordaz, F.J. Alonso, M. Montoto, Manual de Diagnosis y Tratamiento de Materiales Pétreos y Cerámicos, Col.legi d'Aparelladors i Arquitectes Tècnics de Barcelona, Barcelona, Spain, 1997.
- [34] U. Zezza, Physical-mechanical properties of quarry and building stones Pavia (Italy), in: *Advanced workshop "Analytical methodologies for the investigation of damaged stones"*, 1990, p. 21.
- [35] ASTM D2845, Standard Test Method for Laboratory Determination of Pulse Velocities and Ultrasonic Elastic Constant of Rock USA, 2005.
- [36] J. Guydader, A. Denis, Propagation de ondes dans les roches anisotropies sous contrainte évaluation de la qualité des schistes ardoisiers, *Bull. Eng. Geol.* 33 (1986) 49–55.
- [37] UNE-EN 15886, Conservación del patrimonio cultural. Métodos de ensayo. Medición del color de superficies, AENOR, Madrid, Spain, 2011.
- [38] UNE-EN 12370, Métodos de ensayo para piedra natural. Determinación de la resistencia a la cristalización de las sales, AENOR, Madrid, Spain, 1999.
- [39] R.M. Espinosa Marzal, A. Hamilton, M. McNall, K. Whitaker, G.W. Scherer, The chemomechanics of crystallization during rewetting of limestone impregnated with sodium sulfate, *J. Mater. Res.* 26 (2011) 1472–1481.
- [40] Y. Maniatis, M.S. Tite, Technological examination of Neolithic-Bronze Age pottery from central and southeast Europe and from the Near East, *J. Archaeol. Sci.* 8 (1981) 59–76.
- [41] C. Rodriguez Navarro, G. Cultrone, A. Sanchez Navas, E. Sebastián, TEM study of mullite growth after muscovite breakdown, *Am. Mineral.* 88 (2003) 713–724.
- [42] J. Capel, F. Huertas, J. Linares, High temperature reactions and use of Bronze Age pottery from La Mancha, Central Spain, *Miner. Petrogr. Acta* 29A (1985) 563–575.
- [43] M. Dondi, M. Marsigli, B. Fabbri, Recycling of industrial and urban wastes in brick production. A review, *Tile Brick Int.* 13 (1997) 218–309.
- [44] F. Guo, F. Wu, Y. Mu, Y. Hu, X. Zhao, W. Meng, J.P. Giesy, Y. Lin, Characterization of organic matter of plants from lakes by thermal analysis in a N₂ atmosphere, *Sci. Rep.* 6 (2016) 22877, <https://doi.org/10.1038/srep22877>.
- [45] D.L. Whitney, B.W. Evans, Abbreviations for names of rock-forming minerals, *Am. Mineral.* 95 (2010) 185–187.
- [46] M.S. Tite, Y. Maniatis, Examination of ancient pottery using the scanning electron microscope, *Nature* 257 (1975) 122–123.
- [47] A. Cairo, B. Messiga, M.P. Riccardi, Technological features of "Cotto Variiegato": a petrological approach, *J. Cult. Herit.* 2 (2001) 133–142.
- [48] C. Rodriguez Navarro, K. Kudlacz, E. Ruiz Agudo, The mechanism of thermal decomposition of dolomite: new insights from 2D-XRD and TEM analyses, *Am. Mineral.* 97 (2012) 38–51.
- [49] W.A. Tiller, *The Science of Crystallization. Macroscopic Phenomena and Defect Generation*, Cambridge University Press, Cambridge, UK, 1991.
- [50] M. Dondi, G. Ercolani, B. Fabbri, M. Marsigli, Chemical composition of mullite formed during the firing of carbonate rich and iron-containing ceramic bodies, *J. Am. Ceram. Soc.* 82 (1999) 465–468.
- [51] R.E. Kirk, D.F. Othmer, *Encyclopaedia of Chemical Technology*. Vol. 9. Drying, Wiley, New York, 2004, p. 93–141.
- [52] G.W. Scherer, Theory of drying, *J. Am. Ceram. Soc.* 73 (1999) 3–14.
- [53] K.J. Krakowiak, P.B. Lourenço, F.J. Ulm, Multitechnique investigation of extruded clay brick microstructure, *J. Am. Ceram. Soc.* 94 (2011) 3012–3022.
- [54] G. Cultrone, E. Sebastián, K. Elert, M.J. de la Torre, O. Cazalla, C. Rodriguez Navarro, Influence of mineralogy and firing temperature on the porosity of bricks, *J. Eur. Ceram. Soc.* 24 (2004) 547–564.
- [55] N. Saenz, E. Sebastián, G. Cultrone, Analysis of tempered bricks: from raw materials and additives to fired bricks for use in construction and heritage conservation, *Eur. J. Mineral.* 31 (2019) 301–312.
- [56] L. Simonot, M. Elias, Color change due to surface state modification, *Color Res. Appl.* 28 (2002) 45–49.
- [57] J. Molera, T. Pradell, M. Vendrell Saz, The colours of Ca-rich pastes: origin and characterization, *Appl. Clay Sci.* 13 (1998) 187–202.
- [58] A. De Bonis, G. Cultrone, C. Grifa, A. Langella, A.P. Leone, M. Mercurio, V. Morra, Different shades of red: the complexity of mineralogical and physicochemical factors influencing the color of ceramics, *Ceram. Int.* 43 (2017) 8065–8074.
- [59] C.M. Grossi, P. Brimblecombe, R.M. Esbert, F.J. Alonso, Colour changes in architectural limestones from pollution and cleaning, *Color Res. Appl.* 32 (2007) 320–331.
- [60] M. Lassinantti Gualtieri, A.F. Gualtieri, S. Gagliardi, P. Ruffini, R. Ferrari, M. Hanuskova, Thermal conductivity of fired clays: effects of mineralogical and physical properties of the raw materials, *Appl. Clay Sci.* 49 (2010) 269–275.
- [61] R. Saiah, B. Perrin, L. Rigal, Improvement of thermal properties of fired clays by introduction of vegetable matter, *J. Build. Phys.* 34 (2010) 124–142.
- [62] M. Šveda, B. Janík, V. Pavlík, Z. Štefunková, G. Pavlendová, P. Šín, R. Sokolář, Pore-size distribution effects on the thermal conductivity of the fired clay body from lightweight bricks, *J. Build. Phys.* 41 (2017) 78–94.
- [63] K. Elert, G. Cultrone, C. Rodriguez Navarro, E. Sebastian Pardo, Durability of bricks used in the conservation of historic buildings. Influence of composition and microstructure, *J. Cult. Herit.* 4 (2003) 91–99.
- [64] D. Benavente, L. Linares Fernández, G. Cultrone, Influence of microstructure on the resistance to salt crystallization damage in brick, *Mater. Struct.* 39 (2006) 105–113.
- [65] R.J. Flatt, F. Caruso, A.M. Aguilar Sanchez, G.W. Scherer, Chemomechanics of salt damage in stone, *Nat. Commun.* 5 (2014) 4823, <https://doi.org/10.1038/ncomms5823>.
- [66] G.W. Scherer, Crystallization in pores, *Cem. Concr. Res.* 29 (1999) 1347–1358.